

## Nuclear double charge exchange reactions by induced isotensor interactions

H. LENSKE<sup>(1)(2)</sup>, J. BELLONE<sup>(2)</sup>, M. COLONNA<sup>(2)</sup>, D. GAMBACURTA<sup>(2)</sup>  
and JOSE-ANTONIO LAY<sup>(3)</sup> for the NUMEN COLLABORATION

<sup>(1)</sup> *University of Giessen - Giessen, Germany*

<sup>(2)</sup> *INFN, LNS Catania - Catania, Italy*

<sup>(3)</sup> *University of Sevilla - Sevilla, Spain*

received 6 August 2024

**Summary.** — The theory of heavy ion double charge exchange (DCE) reactions is recapitulated with focus on Double Single Charge Exchange (DSCE) and Majorana DCE (MDCE) reactions. DSCE reactions are of second-order distorted wave (DW) character, mediated by isovector nucleon-nucleon (NN) interactions and matrix elements similar to  $2\nu 2\beta$  decay. The MDCE process proceeds by an induced rank-2 isotensor interaction, given by off-shell pion-nucleon scattering, leading to pion potentials similar to the neutrino potentials in  $0\nu 2\beta$  decay.

### 1. – Introduction

As discussed in depth in ref. [1] for a long time heavy ion Double Charge Exchange (DCE) reactions were considered as sequential proton and neutron pair transfers. Only quite recent investigations showed that mesonic DCE reaction mechanisms may prevail under appropriate circumstances, thus giving access to DCE spectroscopy and nuclear matrix elements (NME) of structures as encountered in double beta decay. In this contribution, two competing and interfering reaction mechanisms are discussed, namely nucleon-nucleon (NN) Double Single Charge Exchange (DSCE) and Meson-Nucleon Majorana DCE (MDCE). Connections to double beta decay (DBD) will be pointed out.

### 2. – Double single charge exchange reactions

The DSCE mechanism amounts to a conventional distorted wave two-step reaction. DSCE reactions are a sequence of two single charge exchange events, each of them mediated by the two-body NN-isovector interaction  $\mathcal{T}_{NN}$ , the latter acting by one-body operators on the projectile and the target nucleus, respectively. For a reaction  $\alpha = a(Z_a, N_a) + A(Z_A, N_A) \rightarrow \beta = b(Z_a \pm 2, N_a \mp 2) + B(Z_A \mp 2, N_A \pm 2)$  the reaction

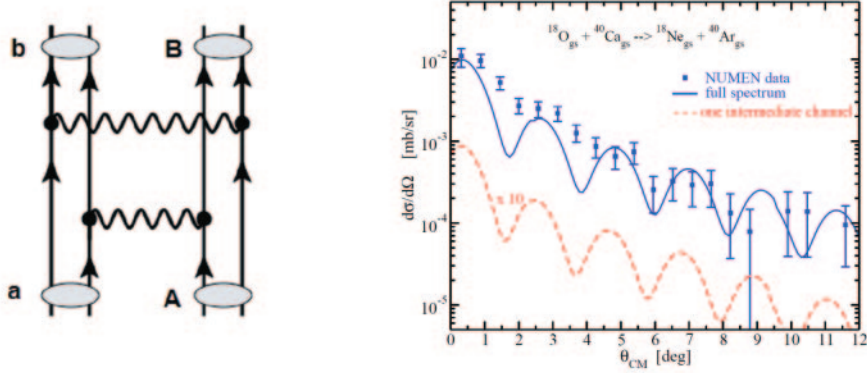


Fig. 1. – DSCE interaction diagram (left) and DSCE angular distribution (right) for  $^{40}\text{Ca} (^{18}\text{O}, ^{18}\text{Ne}_{g.s.})^{40}\text{Ar}_{g.s.}$  at  $T_{lab} = 275$  MeV, compared to the NUMEN data [6]. Intermediate states with angular momenta  $J^\pi = 5^\pm$  are included, the experimental angular resolution of  $\pm 0.6^\circ$  (from [2]) is accounted for. The DSCE cross section obtained by going through only the lowest  $J^\pi = 1^+$  state in  $^{40}\text{K}$  is shown (dashed line).

amplitude is written down readily as a quantum mechanical second order reaction matrix element [2]:

$$(1) \quad \mathcal{M}_{\alpha\beta}^{(2)}(\mathbf{k}_\alpha, \mathbf{k}_\beta) = \langle \chi_\beta^{(-)}, bB | \mathcal{T}_{NN} \mathcal{G}_{aA}^{(+)}(\omega_\alpha) \mathcal{T}_{NN} | aA, \chi_\alpha^{(+)} \rangle.$$

Initial (ISI) and final state (FSI) interactions are taken into account by the distorted waves  $\chi_{\alpha,\beta}^{(\pm)}$ , depending on the invariant center-of-mass (c.m.) momenta  $\mathbf{k}_{\alpha,\beta}$  and obeying outgoing and incoming spherical wave boundary conditions, respectively. The available c.m. energy is  $\omega_\alpha = \sqrt{s_{aA}}$ ,  $s_{aA} = (T_{lab} + M_a + M_A)^2 - T_{lab}(T_{lab} + 2M_a)$ . We use an (anti-symmetrized and complex-valued) isovector NN T-matrix with rank-0 central and rank-2 tensor interactions [3].

Expanding the intermediate many-body propagator  $\mathcal{G}_{aA}^{(+)}$  into the SCE-type states  $\{|c\rangle\}$  and  $\{|C\rangle\}$  in projectile and target nucleus, respectively, one obtains [2, 3]

$$(2) \quad \mathcal{M}_{\alpha\beta}^{(2)}(\mathbf{k}_\alpha, \mathbf{k}_\beta) = \sum_{\gamma=\{c,C\}} \int \frac{d^3k_\gamma}{(2\pi)^3} M_{\gamma\beta}^{(1)}(\mathbf{k}_\gamma, \mathbf{k}_\beta) \frac{\tilde{S}_\gamma^\dagger}{\omega_\alpha - E_c - E_C - T_\gamma(k_\gamma) + i\eta} M_{\alpha\gamma}^{(1)}(\mathbf{k}_\alpha, \mathbf{k}_\gamma),$$

where  $E_{c,C} = M_{c,C} + T_{c,C}$  are the total c.m. energies of the intermediate states.  $T_\gamma$  denotes the kinetic energy related to the (off-shell) momentum  $k_\gamma$ .  $M_{\alpha\gamma}^{(1)}(\mathbf{k}_\gamma, \mathbf{k}_\alpha)$  are the – half off-shell – SCE-amplitudes.  $\tilde{S}_\gamma^\dagger \sim \langle \tilde{\chi}_\gamma^{(+)} | \tilde{\chi}_\gamma^{(-)} \rangle$  is the dual S-matrix element related to the non-hermitian Hamiltonian of relative motion [2, 4, 5].

In fig. 1 the theoretical DSCE cross section is compared to the measured DCE angular distributions for the reaction  $^{40}\text{Ca} (^{18}\text{O}, ^{18}\text{Ne})^{40}\text{Ar}$  at  $T_{lab} = 275$  MeV [6]. A large spectrum of intermediate states up to  $J^\pi = 5^\pm$  was included. The magnitude of the measured cross section is almost perfectly well reproduced without the need for adjustments by scaling factors.

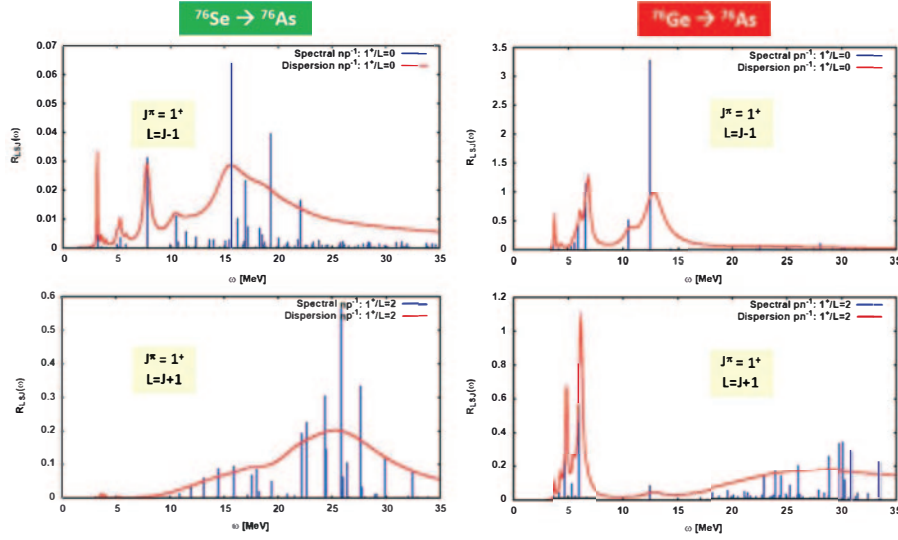


Fig. 2. – QRPA response functions for  $^{76}\text{Se}_{g.s.}(0^+) \rightarrow ^{76}\text{As}(1^+)$  (left) and  $^{76}\text{Ge}_{g.s.}(0^+) \rightarrow ^{76}\text{As}(1^+)$  (right), using the multipole operators  $T_{(LS)JM} = \left(\frac{r}{R}\right)^L [i^L Y_L(\hat{r}) \otimes \sigma]_{JM} \tau^\pm$ ,  $R = 1.2A^{1/3} \simeq 5.08$  fm. The self-consistent HFB-plus-QRPA approach of ref. [8] is used with a discretized continuum in a cavity of radius  $R_C = 120$  fm. Results of a conventional spectral QRPA calculation (discrete lines) and an extended QRPA approach including dispersive self-energies are compared. Summation of the  $L = J - 1 = 0$  strengths up to  $\omega = 60$  MeV, the Ikeda sum rule is  $S_{GT}(-) - S_{GT}(+) = 33.96 < 3(N - Z) = 36$ .

As explained in detail in ref. [7] contour integration techniques and a considerable amount of angular momentum recoupling allow to separate projectile and target NME's. As a result, rank-2 nuclear polarization tensors are obtained,

$$(3) \quad \Pi_{(S_1 S_2) SM}^{(AB)}(\mathbf{p}_2, \mathbf{p}_1; \omega) = \sum_C \frac{\left[ F_{S_2 T}^{(BC)}(\mathbf{p}_2) \otimes F_{S_1 T}^{(CA)}(\mathbf{p}_1) \right]_{SM}}{\omega - (E_A - E_C)},$$

describing the nuclear response for total spin transfer  $\mathbf{S} = \mathbf{S}_1 + \mathbf{S}_2$ . The striking formal similarity to the NME of  $2\nu 2\beta$  decay is obvious.

In practice, the response tensors are calculated in Quasiparticle Random Phase Approximation (QRPA) [3, 8]. Spectral distributions for the reaction shown in fig. 1 are found in [2]. In fig. 2 QRPA response functions for  $A = 76$  nuclei, which are of equally high interest for DCE and DBD investigations, are displayed. As representative examples, the  $J^\pi = 1^+$  Gamow-Teller response functions for  $^{76}\text{Se}_{g.s.}(0^+) \rightarrow ^{76}\text{As}(1^+)$  and  $^{76}\text{Ge}_{g.s.}(0^+) \rightarrow ^{76}\text{As}(1^+)$  are compared for both orbital angular momentum transfers,  $L = J \pm 1 = 0, 2$ . First of all, it is seen that the shape and strength of spectral distributions depend considerably on the parent system. Secondly, it is of interest that in both the  $\tau^\pm$  directions a high lying Gamow-Teller resonance with  $L = J + 1 = 2$  around  $\omega \sim 25$  MeV appears which is not contained in the  $L = J - 1 = 0$  sub-channel response.

### 3. – The isotensor Majorana DCE mechanism

If two nuclei are in close contact as in a peripheral ion–ion collision, an effective isotensor interaction can be generated dynamically. This case is investigated by the Majorana DCE (MDCE) reaction scenario [1, 5]. As illustrated in fig. 4, the MDCE mechanism amounts to a pair of virtual ( $\pi^\pm \rightarrow \pi^0 \rightarrow \pi^\mp$ ) reactions. The reacting nuclei interact by the  $t$ -channel exchange of charged pions. A typical scenario is a  $\pi^\pm \rightarrow \pi^0$  reaction, inducing SCE–type transitions  $A(Z, N) \rightarrow C(Z \mp 1, N \pm 1)$ , followed by  $\pi^0 \rightarrow \pi^\pm$  conversion in a second SCE-transition  $C(Z \mp 1, N \pm 1) \rightarrow B(Z \mp 2, N \pm 2)$ . In total, an off-shell ( $\pi^+, \pi^-$ ) reaction in one nucleus is accompanied by a complementary ( $\pi^-, \pi^+$ ) reaction in the other nucleus.

MDCE is described by the box diagrams shown in fig. 4. The MDCE operator induces two–particle–two–hole ( $p^2n^{-2}$ ) and ( $n^2p^{-2}$ ) DCE transitions, respectively. When replacing in the MDCE graph of fig. 4 the neutral pions ( $\sim q\bar{q}$ ) by a pair of Majorana neutrinos  $\nu\bar{\nu}$  and the charged pions by charged leptons, the remarkable topological similarity to  $0\nu 2\beta$  decay is recognized. Although the MDCE and DBD transition operators are not fully identical, they probe the same transitions and wave functions.

MDCE pion–nucleon dynamics is completely different from the DSCE NN–interactions. In the energy region relevant for the MDCE process the (off-shell) isovector pion–nucleon T-matrix  $T_{\pi N}$  is described adequately by the operator structure

$$(4) \quad \mathcal{T}_{\pi N} = \left[ T_0 + \frac{1}{m_\pi^2} (T_1 \mathbf{p} \cdot \mathbf{p}' + iT_2 \boldsymbol{\sigma} \cdot (\mathbf{p} \times \mathbf{p}')) \right] \mathbf{T}_\pi \cdot \boldsymbol{\tau}_N.$$

The energy–dependent vertex form factors  $T_{0,1,2}$  are determined by  $\pi N$  S– and P–wave interactions, dominated by the formation of  $N^*$  resonances of isospin  $I = \frac{1}{2}, \frac{3}{2}$ .  $T_0$  is given by S–wave resonances with  $J^\pi = \frac{1}{2}^-$ , while for  $T_{1,2}$  P–wave resonances,  $J^\pi = \frac{1}{2}^+, \frac{3}{2}^+$ , are essential, including, *e.g.*,  $\Delta_{33}(1232)$  and the Roper resonance  $P_{11}(1440)$ . Convergence of the (off–shell) interactions is achieved by including resonances up  $M_{N^*} \sim 1800$  MeV.

The key elements for spectroscopy are the nuclear matrix elements  $\mathcal{W}_{AB} = \mathcal{W}_{12}$  and  $\mathcal{W}_{ab} = \mathcal{W}_{34}$ , describing the vertical left and right branches, respectively, of the graph shown in fig. 4. They depend on the external momenta  $\mathbf{p}_{1,2}$  attached to the charged pions. The MDCE transition form factor is given by

$$(5) \quad \mathcal{W}_{AB}(\mathbf{p}_1, \mathbf{p}_2) = - \sum_C \int \frac{d^3k}{(2\pi)^3} \mathcal{M}_{BC}(\mathbf{p}_2, \mathbf{k}) \frac{1}{k^2 + m_\pi^2 - \omega_{CA}^2} \mathcal{M}_{CA}(\mathbf{k}, \mathbf{p}_1),$$

where the summation extends over the intermediate SCE–type configurations  $C$ . The two charge–converting processes are described by  $\mathcal{M}_{CA}(\mathbf{k}, \mathbf{p}) = \langle C | e^{i\mathbf{q}_i \cdot \mathbf{r}} \tilde{\mathcal{T}}_{\pi N}(\mathbf{k}, \mathbf{p}) | A \rangle$  and correspondingly for  $\mathcal{M}_{BC}$ .

The pion rest mass  $m_\pi \sim 139$  MeV defines a natural separation scale allowing to evaluate the NME safely in closure approximation, by which we obtain the pion potential [1]

$$(6) \quad \mathcal{U}_\pi(\mathbf{x} | \mathbf{p}_{1,2} \boldsymbol{\sigma}_{1,2}) = - \int \frac{d^3k}{(2\pi)^3} T_{\pi N}(\mathbf{p}_2, \mathbf{k} | \boldsymbol{\sigma}_2) \frac{e^{i\mathbf{k} \cdot \mathbf{x}}}{k^2 + m_{\pi^0}^2} T_{\pi N}(\mathbf{p}_1, \mathbf{k} | \boldsymbol{\sigma}_1).$$

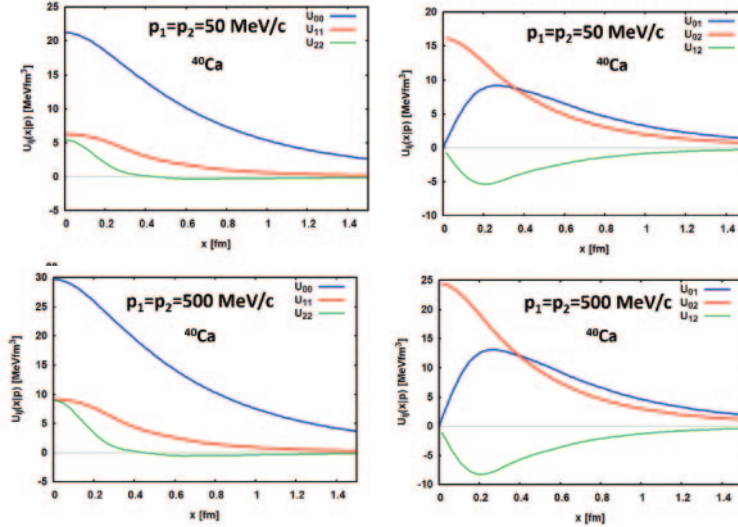


Fig. 3. – The MDCE pion potentials for collinear  $\mathbf{p}_1 \parallel \mathbf{p}_2$  momenta at  $p_1 = p_2 = 50 \text{ MeV}/c$  (upper row) and  $p_1 = p_2 = 500 \text{ MeV}/c$  (lower row). Integrals are regularized by dipole form factors with a hard cut-off  $\Lambda = 2000 \text{ MeV}/c$ . Angular integrations can be carried out in closed form. The remaining  $k$ -integrals, given by products of ordinary or spherical Bessel functions, respectively, and Legendre functions of the second kind multiplied by powers of  $k$ , have to be evaluated numerically.

The (two-body) transition form factor becomes

$$(7) \quad W_{AB}(\mathbf{p}_1, \mathbf{p}_2) = -\langle B | e^{-i\mathbf{p}_2 \cdot \mathbf{r}_2} \mathcal{U}_\pi(\mathbf{x} | \mathbf{p}_{1,2} \sigma_{1,2}) e^{i\mathbf{p}_1 \cdot \mathbf{r}_1} \mathcal{T}_{2\pm 2} | A \rangle,$$

including the rank-2 isotensor  $\mathcal{T}_{2\pm 2} = [\boldsymbol{\tau}_1 \otimes \boldsymbol{\tau}_2]_{2\pm 2}$ .

$\mathcal{U}_\pi(\mathbf{x})$  consist in general of nine terms, reducing in collinear kinematics  $\mathbf{p}_1 \parallel \mathbf{p}_2$  to six independent scalar form factors,  $U_{ij}(x|p_1, p_2) \sim T_i T_j$ ,  $i \leq j = 0, 1, 2$ . Typical results for  $U_{ij}$  are shown in fig. 3. The S-wave terms  $U_{00} \sim T_0^2$  dominate the diagonal potentials, but the mixed S-/P-wave components  $U_{0j}$  ( $j = 1, 2$ ) are of comparable magnitude. This has important implications for future spectroscopic studies, because both non-spin-flip Fermi-type transitions and spin-flip Gamow-Teller-type modes as well as mixed transitions will be excited in MDCE reactions.

The s-channel  $\pi^0$  exchange between the two intranuclear interaction vertices establishes a two-nucleon short-range correlation where the correlation lengths never exceeds 40% of the range of pion exchange. First preliminary results, neglecting the non-diagonal pion potentials and not taking into the coherence of the MDCE and the DSCE reaction amplitudes, are shown in fig. 4. Remarkably, the angular region of fig. 4 covers momentum transfers up to  $500 \text{ MeV}/c$ .

#### 4. – Summary

A fully microscopic theory of heavy ion DCE reactions was presented, including sequential DSCE and direct MDCE contributions. The DSCE amplitude is of a in principle

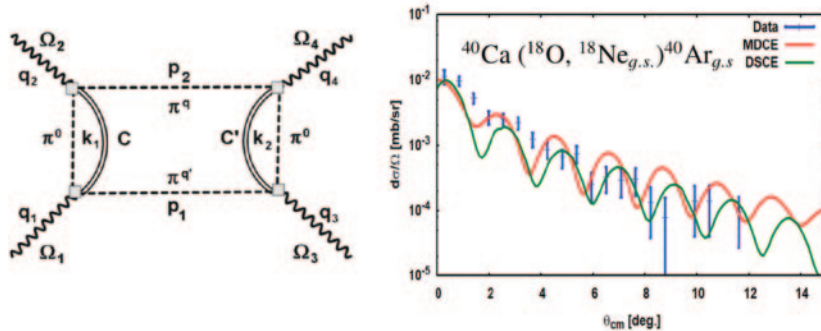


Fig. 4. – The MDCE box diagram (left) and the DSCE and MDCE cross sections compared to the NUMEN data for  $^{40}\text{Ca}(^{18}\text{O}, ^{18}\text{Ne}_{g.s.})^{40}\text{Ar}_{g.s.}$  at  $T_{lab} = 275$  MeV [6]. The MDCE cross section is evaluated in closure approximation and contains only contributions from the diagonal pion potentials, also being normalized arbitrarily to the forward angular distribution. Results are folded with the experimental angular resolution of  $\pm 0.6^\circ$ .

well known two-step structure. The MDCE process, however, relies on a hitherto unknown mechanism, namely a dynamically induced rank-2 isotensor interaction. The DSCE nuclear matrix elements are given by nuclear polarization tensors, occurring also in  $2\nu 2\beta$  decay. In MDCE closure approximation, pion potentials and nuclear matrix elements are obtained close to those encountered in  $0\nu 2\beta$  decay. In principle, the MDCE process can also proceed by rho-mesons or a combination of pions and rho-mesons. However, explicit calculations show that pion-MDCE dominates by far.

\* \* \*

Support by DFG, grant Le439/16 and INFN-LNS Catania is gratefully acknowledged.

## REFERENCES

- [1] CAPPUZELLO F. *et al.*, *Prog. Part. Nucl. Phys.*, **128** (2023) 103999.
- [2] BELLONE JESSICA I., BURRELLO STEFANO, COLONNA MARIA, LAY JOSE-ANTONIO and LENSKE HORST, *Phys. Lett. B*, **807** (2020) 135528.
- [3] LENSKE HORST, BELLONE JESSICA I., COLONNA MARIA and LAY JOSE-ANTONIO, *Phys. Rev. C*, **98** (2018) 044620.
- [4] LENSKE HORST, *Int. J. Mod. Phys. E*, **30** (2021) 2130010.
- [5] LENSKE H., CAPPUZELLO F., CAVALLARO M. and COLONNA M., *Prog. Part. Nucl. Phys.*, **109** (2019) 103716.
- [6] CAPPUZELLO F., CAVALLARO M., AGODI C., BONDI M., CARBONE D., CUNSOLO A. and FOTI A., *Eur. Phys. J. A*, **51** (2015) 145.
- [7] LENSKE HORST, BELLONE JESSICA, COLONNA MARIA and GAMBACURTA DANILO, *Universe*, **7** (2021) 98.
- [8] LENSKE HORST and TSONEVA NADIA, *Eur. Phys. J. A*, **55** (2019) 238.